Proceedings of BS2013:
13th Conference of International Building Performance Simulation Association, Chambéry, France, August 26-28

EXPERIMENTATION AND MODELLING OF A SMALL-SCALE ADSORPTION COOLING SYSTEM IN TEMPERATE CLIMATE

Sébastien Thomas[1], Samuel Hennaut[1], Stefan Maas[2] and Philippe André[1]

[1]University of Liège, Arlon, Belgium

[2]University of Luxembourg, Luxembourg

July 22, 2013

ABSTRACT

This paper describes the results of monitoring campaigns of a solar driven adsorption air-conditioning system. The energy performance figures of the system are computed and the adsorption chiller is modelled also based on measurement. This renewable energy system is able to reach, on a monthly cooling period, 40% energy savings compared to a classical air-conditioning system. Besides, the model built to handle the adsorption thermal behaviour shows performance slightly lower than the manufacturer's performance map.

INTRODUCTION

A small-scale adsorption chiller has been installed in a laboratory building in 2011 in Arlon (South of Belgium). This building was previously equipped with a fully monitored heat and cold production and distribution system. Besides, a solar collector field is used for building heating and domestic hot water production. The building has the shape and size of a small residential house. The solar cooling system common ratio between solar collector size and cooling power ranges from 2.5 to 3.5 m^2/kW_C (Henning, 2007). The installed system has 14 m^2 solar collector for a nominal cooling power of $9kW_C$ (1.55 m^2/kW_C). Both economical and architectural limits made difficult to enlarge the existing solar collector field. Some electrical resistances are set up to compensate the lack of collectors.

Installed system

The general scheme of the installed system is displayed on figure 1. By operating and measuring this cooling system in real scale conditions, it is proposed to assess its thermal and electrical performance. The main components dedicated to solar air-conditioning are listed below (from left to right on figure 1):

- The hot water loop containing flat-plate solar collectors and hot water storage (300 litres with 7.2 kW electrical heater). The South roof has an azimuth of 43° to East and a slope of 42°.
- The adsorption chiller (ADS) containing two reactors with total cooling nominal power 9 kW_C
- The recooling loop and its dry cooling tower
- The cold water loop including the cold water storage (500 litres)
- Cold emission devices for cooling the laboratory building: cooling floor, cooling ceiling, air handling unit

Chiller selection

The selected sorption chiller has to satisfy some requirements in order to be installed in the laboratory building:

- An appropriate cooling power to meet the building cooling load($<$ 10 kW)
- Good performance at part load conditions
- Low driving temperature due to the collectors technology

Through the market available thermally driven cooling solutions, an adsorption chiller with zeolithe-water couple has been selected to satisfy the previous requirements. It has two adsorbers operating in phase opposition. Moreover, the thermal COP given by the manufacturer keeps high value even with low driving temperature (INVENSOR, 2010). For example, the announced thermal COP is 0.55 for 60°C driving heat, 27°C recooling and 18°C cooling water (chiller inlets). This chiller can reach up to 8°C cold water but it is usually operated with cold water from 15-18°C to reach better performance. It is mainly used in combination with cooling ceiling or floors.

SYSTEM MONITORING

Some measurement must be achieved to compute the energy performances indexes. The relevant energy flows (heat, cold, electricity...) are computed based on measurement to be able to derive key figures such as thermal COP, electrical COP...The measurements picked up every 10 seconds in the installed solar air-conditioning system enable the computation of those indexes.

The building is considered as an infinite heat source, the whole cold energy produced can be consumed by the building. This is the reason why the adsorption cooling system monitoring focuses on cold production, the measurements on the cold distribution or emission are not presented in this work.

The probes can be split into three groups: thermal, electrical measurements and meteorological data. The table 2 describes the main computations based on temperatures, flows and power measurements. The hydraulics module includes the three pumps feeding the adsorption chiller. The distribution pump on building side is not taken into account as it would have been present whatever the cooling system installed. The deduced accuracy mentioned is based on the temperatures probes and mass flow meter specifications. The heat flow balance ($Q_{rej} - Q_{heat} - Q_{cold} = 0$) is nearly met on a daily basis. The heat flow and thermal COP error listed in table 2 are consequently a little bit pessimistic.

MONITORING RESULTS

The testing period (36 days from June to August 2012 - representative of a summer period in Belgium) analysed in this work copes with emulated solar collector. As mentioned before, the available collector surface on the laboratory roof is not sufficient to run the adsorption chiller in nominal operation. It is proposed to use the 14 m^2 solar collector and add 14 m^2 emulated collectors with electrical resistances. Their control allows to add the same amount of thermal energy as that provided by the collector. The chiller operation handles real scale conditions driven by a combination of real and emulated collectors.

Energy performance indexes

For comparison purpose, some solar driven air-conditioning system energy indexes have been developed (Nowag et al. (2012) and Napolitano et al. (2011)). Here are the definitions of those ratios suited to the studied system. They can be computed on any time basis. The collector yield is expressed in equation 1. The chiller thermal behaviour is characterized by the thermal Coefficient Of Performance (equation 2). The electricity consumption is crucial to assess the solar air-conditioning systems performance (Thomas and André, 2012), $COP_{elec\,tot}$ (equation 3) depicts the cold energy produced in relation to the total electricity consumed. This does not consider the electrical resistances emulating the collectors, but includes twice the real collector pump to consider the electricity that would have been paid to drive the thermal flow from collectors to the hot water storage. The electrical performances of the solar loop and cooling tower are respectively defined in equations 4 and 5, they represent the useful energy flow divided by the device electrical consumption. To compare the energy performance with a conventional electricity driven vapour compression chiller, the fraction of energy savings (f_{sav}) is defined in equation 6 (where 2.8 is the seasonal COP of a reference vapour compression chiller).

$$\eta_{thermal\ collector} = \frac{Q_{coll}}{Q_{sol}} \quad (1)$$

$$COP_{Therm} = \frac{Q_{cold}}{Q_{heat}} \quad (2)$$

$$COP_{elec\,tot} = \frac{Q_{cold}}{Qe6 + 2 * Qe7 + Qe8} \quad (3)$$

$$COP_{solar\ loop} = \frac{Q_{coll}}{Qe7} \quad (4)$$

$$COP_{rej} = \frac{Q_{rej}}{Qe8} \quad (5)$$

$$f_{sav} = 1 - \frac{COP_{elec\,tot}}{2.8} \quad (6)$$

Global results

Table 1: Solar cooling installation key indexes for 36 days summer period

Q_{cold} [kWh/day]	19.7
$\eta_{thermalcollector}$	0.31
COP_{Therm}	0.55
$COP_{elec\,tot}$	4.69
$COP_{solar\ loop}$	38.58
COP_{rej}	57.50
f_{sav}	0.40

The indexes computed for this period can be found in table 1 (left column). As mentioned before, the cooling system cools an infinite load, it starts if the hot storage tank reaches 65°C and stops if it drops below 55°C. The cold water from storage tank ranges from 15-18°C. The rejection temperature is controlled via the fans to reach 27°C as chiller inlet temperature.
The mean daily cold energy produced is around 20 kWh. Besides, it has a daily high variability (0 - 38.2 kWh) due to the solar radiation (only energy source). This system could be coupled to a building where the load is mainly influenced by the solar radiation otherwise a back-up system must be installed.
The thermal collector efficiency is 31%, it is a common encountered value for collector summer operation. The flat-plate collectors have a lower yield because of high operating temperature. Clouds are often presents in the Belgian sky, the diffuse radiation is not high enough to operate the collectors at high temperatures. These two reasons explain mainly the apparently low thermal yield value. The sunnier days show slightly better yields up to 45%.
The thermal COP reaches nearly the chiller nominal value, it shows a global good energy performance despite the low driving temperatures. The system satisfies the minimal requirements mentioning the mean COP should be higher than 0.8 times the nominal COP (Nowag et al., 2012).
The electrical performance is depicted by the electrical COP. The solar air-conditioning system electrical COP ($COP_{elec\,tot}$) does not meet at all the targeted value of 10 (Wiemken et al., 2010). The electricity sharing is measured as follows: collector pump 28%,

cooling tower 21%, chiller and pumps 51%. Besides, the stand by consumption is about 30 W for the adsorption chiller and the cooling tower. It counts for 17% of the total electricicty consumption for the period.

The rejection COP (COP_{rej}) details the cooling tower performance which is strongly linked with the external temperature. A hot day shows an electricity consumption ratio five times higher compared to a sunny day with lower ambient temperature. The ambient temperatures met during this period were quite low, 29.7°C was the maximum measured.

In spite of the low electrical performance, some energy savings are encountered compared to a classical air conditioning system. This system reaches 40% energy savings (f_{sav}) on the whole period.

ADSORPTION CHILLER MODELLING

The monitoring results emphasize the performance of adsorption chiller regarding the inlet temperatures and also showed a different thermal behaviour occurring at start-up. The adsorption chiller has an intermittent operation, the refrigerant goes successively through four steps: adsorption, desorption, evaporation, condensation (Wang and Oliveira, 2006). This paragraph explains the thermal modelling of the adsorption chiller itself. The analysis is tackled with heat flows measurement outside the machine to determine its thermal COP and the cooling capacity. The objective is to create a simple model to evaluate as accurately as possible the thermal performance of the adsorption chiller. It could be used afterwards in energy simulation software to evaluate a solar cooling system performance throughout the cooling season.

Existing adsorption chiller models

The existing simulation models for adsorption chiller can be separated into two categories Döll (2011):

- Dynamic models that try to represent the actual physical phenomena inside the machine as described by Schicktanz et al. (2012) or Wang and Chua (2007)
- Static models that simplify the physical phenomena (they are often using performance map) as described by Albers and Römmling (2002)

Both approaches have their drawbacks. Since dynamic models can reveal the real adsorption phenomenon, they can be used for optimization of operation or materials characteristics evaluation. Those models are generally high computer resources consuming which makes annual system simulation infeasible. The static models are less accurate and do not take any dynamic effect into account. Yearly simulations with static models overestimate commonly the energy performance of systems (Thomas et al., 2012).

New adsorption chiller model

The idea of the new model developed in the following paragraphs is to take the dynamic of the system in a long time scale (longer than cycle duration) into account and avoid short time dynamics (shorter than cycle duration). One cycle has its own dynamics, it is repeated each time. The energy flows through one cycle are represented on the figure 2, it is proposed to create a model based on mean half-cycle values.The model is based on measurements and not on the machine physical properties; it could be exploited only for the same kind of machine. The main assumptions for this model are listed below:

- The thermal behaviour of the adsorption chiller can be split into two modes: start-up and steady-state
- Inlet temperatures are nearly constant throughout the half-cycle
- There is no mass flow modifications (the nominal mass flow are used)
- The steady-state half-cycles are only influenced by the previous half-cycle

The last assumption needs more explanations: one cycle entails the succession of heating and cooling of an adsorber, there is no energy storage on longer time scale. The cold energy produced during the adsorption phase depends on the cold water inlet temperature and recooling inlet temperature **within this phase** and on the hot water temperature charging the adsorber during **the two previous phases**. This interpretation leads to forget all information about cycle operation before the adsorber previous loading to model the adsorption chiller. This assumption is not taken for the chiller start-up because it handles the first charge of the adsorbers. The model proposes on the one hand a performance map of cooling capacity and heat input (thermal COP can be deducted) for the chiller in steady-state operation. That will be compared to the manufacturer static performance map. On the other hand, it should give coefficients to modify the performance map to handle the start-up period.

Data processing

It has been decided to use mean half cycle measurements. To split the data into half cycles the rejection heat flow peak is taken as the beginning. It corresponds respectively to the beginning of adsorption and desorption phases of the two adsorbers.

Steady-state operation modelling

First of all, it is important to distinguish the beginning period and the steady-state one. To do this, the comparison is achieved between measured thermal COP and manufacturer steady-state performance curves. The beginning period stands for measurements that do not meet the manufacturer's data at all: 10 minutes is kept as beginning period, it is avoided in the steady-state analysis.

These half-cycles are used in the steady-state analysis, this represents 1700 half-cycles:

- They begin at least 10 minutes after chiller start-up (steady-state operation)
- They have mean driving temperature between 55 and 75°C (consistent with the manufacturer temperature range)
- They have slight hot temperature variation through the cycle < 4°C (consistent with mean temperature hypothesis)
- They don't have too low cold inlet temperature >10°C (consistent with the manufacturer temperature range)

The manufacturer model gives good agreement with the mean measured COP on the total measurement period (2.4% error with mean thermal COP = 0.574). Besides, the standard deviation of thermal COP variation (manufacturer and measured) is quite high. The error is much more important on cooling capacity, the measured one is 30% lower than the manufacturer model. Two modes are emphasized: short cycles ($<$ 10 minutes) when the cold supply temperature is above 17°C and long cycles (20 minutes) in other cases. The **short cycles represent full load** chiller operation while the **long cycles represent part load** operation. Due to the cold water set point of 15°C, the adsorption chiller operates at part load conditions if the chiller cold water inlet temperture drops below 17°C. The two operation modes have considerable differences, thus two models must be set up to handle the both cases.

The model is a correlation between the cold energy measured and some other measured variables that do not directly depend on chiller behaviour. Those variables are the mean chiller inlet temperatures in current half-cycle or previous half-cycles. Moreover, they include the difference between those temperatures levels. A stepwise linear regression is achieved with those variables. The two most significant variable to explain the cold energy produced are the chiller inlet mean hot water temperature at previous half-cycle $T_{H\ in\ mean\ -1}$ and the difference between mean inlet rejection and cold temperature at current time step $(T_{R\ in\ mean} - T_{C\ in\ mean})$. This corroborates the influence of the previous cycle on cold production. The heat energy input most significant variables are $T_{H\ in\ mean}$ (current half-cycle) and $(T_{R\ in\ mean} - T_{C\ in\ mean})$. The rejection temperature did not vary a lot around 27°C, the analysis is only valid for mean chiller inlet rejection temperatures ranging from 26°C to 29°C. The relatively low upper bound is due to the low ambient temperature during the testing period while the lower bound is a consequence of the fan control trying to reach 27°C.

Knowing the important variables, it is now interesting to investigate the correlation functions. Taking the theoretical sorption cycle into account (Wang and Oliveira, 2006), the cold production depends on the amount of sorbent adsorbed. The x-axis of Oldham diagram is in fact $-1/T$ while the pressure depends on the temperature with an exponential law. The best estimation of the cold and heat production (least squared method) is given by the functions detailed in equations 7 and 8 where the temperature stand in °C.

$$\begin{aligned}\dot{Q}_C = {} & a \cdot exp(b + c \cdot T_{H\ in\ mean\ -1}) \\ & + \frac{d}{T_{H\ mean\ -1}} + \frac{e}{T^2_{H\ in\ mean\ -1}} \\ & + \frac{f}{(T_{R\ in\ mean} - T_{C\ in\ mean})} + g\ [kW]\end{aligned} \tag{7}$$

$$\begin{aligned}\dot{Q}_H = {} & a \cdot exp(b + c \cdot T_{H\ in\ mean}) \\ & + \frac{d}{T_{H\ mean}} + \frac{e}{T^2_{H\ in\ mean}} \\ & + \frac{f}{(T_{R\ in\ mean} - T_{C\ in\ mean})} + g\ [kW]\end{aligned} \tag{8}$$

The coefficient of the model are given in table 3. The error is also mentioned (Root Mean Squared Error) for both sets of data. 80% of the data is used for building the model while 20% is used for testing it. The seasonal error describes the total error on the whole test.

The graphical view of equations 7 and 8 is then displayed on figure 3 for the two models: short and long cycles. Moreover, the ratio of cooling capacity and heat energy input functions (thermal COP) curve is mentioned. This last curve considers $T_{H\ in\ mean\ -1}$ equals $T_{H\ in\ mean}$. This figure reveals the influence of the hot water inlet temperature on the cold production. For the long cycles the maximum cold energy produced is encountered for inlet temperature near 68°C, the distance between ">5 kW" curves decreases as much as the temperature gap between rejection and cold flows increases (the chiller has to fill a higher temperature gap between condenser and evaporator). Besides, for long cycles, the thermal performance of the machine is quite constant (thermal COP > 0.5) over the entire temperature range while it varies a lot for short cycles. To attain a thermal COP of 0.5, hot source should reach 61-63°C.

Figure 3 also shows the measured half-cycles (blue points). This details the representativeness of the model. Much more long half-cycles have been recorded (right graphs). It gives in table 4 the new created model validity temperature ranges. Unfortunately, the new model cannot describe the chiller energy performance on the whole temperature range. In comparison with the manufacturer's data, high hot water temperature combined with high cold water temperature is not handled in the new model. However, low cold water temperature operation is wider handled in the new model.

The comparison between manufacturer's data and the model gives the curves showed on figure 4. As mentioned below, the validity range of model is restricted to the measured half-cycles. So, for short cycles (Inlet temperature > 17°C), there are no measurement above 65°C.

The tendency of manufacturer curve is confirmed by the new model based on measurement. The two operation mode long and short cycles give respectively good agreement with cooling capacity and thermal COP. However, measured short cycle operation has globally a thermal COP decreased by 0.06 compared to manufacturer's data. Concerning the cold power of long cycle operation, it is decreased by around 1 kW (meaning the available cold power decrease by using the part load operation). These are significant differences between the manufacturer and measurement approach.

The difference can be partially explained by the measurement procedure. The probes for temperature measurements are located at the bounds of hydraulics module while the manufacturer curve deals only with the chiller itself. Our measurements include losses in the hydraulics module and the thermal influence of pumps. Nevertheless, the impact is not important: the hydraulics module is well insulated and pumps for hot and cold loops consume less than 150W each. What is measured in our case is the real energy flow consumed/produced by the system (including chiller and hydraulics module). The measurement error could also assume the differences between manufacturer's data and measured points even though no bias has been encountered in the energy flow measurements.

Start-up operation modelling

The start-up period entails uncommon half-cycles. The shape of the energy flows can be different each time the chiller starts. A model used to compute the energy performance in this crucial part of the chiller operation will be available soon. It will give adjustment coefficients to modify the steady-state model to handle the start-up operation.

CONCLUSION

This paper has shown the results of a small scale solar cooling system experimentation. On one hand, the computation of global indexes for the cooling period has achieved high performance, fraction of energy savings remains high (40%) but is greatly affected by the external temperature (influencing heat rejection electrical COP). On the other hand, a steady-state model has been developed based on half-cycle mean measurement. The low error between model and measurement supports the assumptions made: the chiller thermal behaviour is only influenced by the current and previous half-cycle heat flows. Two operation modes depending on the chiller are emphasized: short cycles for full load operation and long cycles for part load operation. The model has been compared to the manufacturer's data with good agreement for thermal COP or cold production for respectively long and short cycles. Some measurements with both high inlet temperature cold temperature ($>17°C$) and high inlet hot temperature ($>65°C$) should be provided to enlarge the model temperature validity range.

REFERENCES

Albers, J. and Römmling, U. 2002. Trnsys type107 part load simulation of single staged absorption chillers in quasi steady states. Technical report, IEA SHC TASK25 Subtask B.

Döll, J. 2011. Simulation of adsorption chiller using artificial neural networks. In *Proceedings of the 4th International Conference Solar Air-Conditioning, Larnaca, Cyprus*.

Henning, H. 2007. *Solar-assisted air conditioning in buildings: a handbook for planners*. Springer.

INVENSOR 2010. Adsorption chiller invensor ltc 09. Technical report, INVENSOR COMPANY.

Napolitano, A., Sparber, W., Thür, A., Finocchiaro, P., and Nocke, B. 2011. Monitoring procedure for solar cooling systems. Technical report, Task 38 Report, Solar Air-Conditioning and Refrigeration.

Nowag, J., Boudéhenn, F., Denn, A. L., Lucas, F., Marc, O., Raduslescu, M., and Papillon, P. 2012. Calculation of performance indicators for solar cooling, heating and domestic hot water systems. *Energy Procedia*, 30(0):937 – 946.

Schicktanz, M., Hügenell, P., and Henninger, S. 2012. Evaluation of methanol/activated carbons for thermally driven chillers, part ii: The energy balance model. *International Journal of Refrigeration*, 35(3):554 – 561.

Thomas, S. and André, P. 2012. Numerical simulation and performance assessment of an absorption solar air-conditioning system coupled with an office building. *Building Simulation*, 5 Issue 3:243–255.

Thomas, S., Hennaut, S., Maas, S., and André, P. 2012. Experimentation and simulation of a small-scale adsorption cooling system in temperate climate. *Energy Procedia*, 30:704 – 714.

Wang, R. and Oliveira, R. 2006. Adsorption refrigeration - an efficient way to make good use of waste heat and solar energy. *Progress in energy and combustion science*, 32:424–458.

Wang, X. and Chua, H. T. 2007. Two bed silica gel-water adsorption chillers: An effectual lumped parameter model. *International Journal of Refrigeration*, 30:1417–1426. 0140-7007 doi: 10.1016/j.ijrefrig.2007.03.010.

Wiemken, E., PetryElias, A., Wewior, J., Koch, L., and Nienborg, B. 2010. Performance and perspectives of solar cooling. In *Proceedings of Eurosun 2010, International Conference on Solar Heating, Cooling and Buildings, Graz, Austria*.

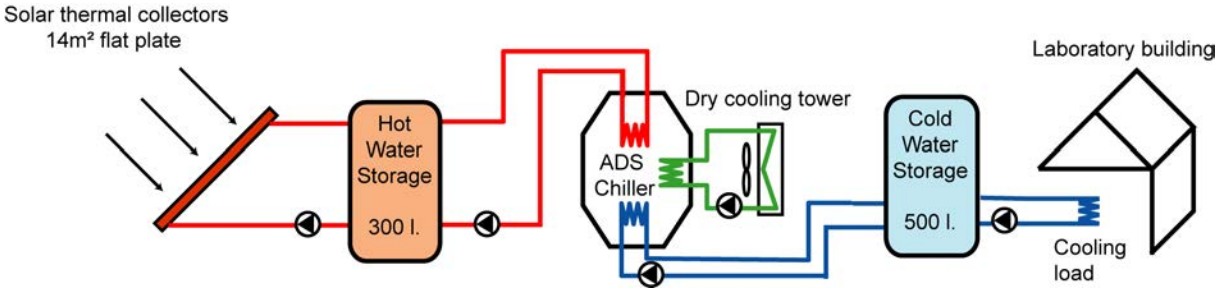

Figure 1: Installed adsorption cooling system scheme

Table 2: Energy flows measurement and their accuracy

Thermal flows	**Variable name**	**Unit**	**Accuracy**
Chiller heat consumption	$\dot{Q}_{heat}$	[kW]	9% +/- 1.08 [kW]
Chiller heat rejected	$\dot{Q}_{rej}$	[kW]	12% +/- 2.13 [kW]
Chiller cold produced	$\dot{Q}_{cold}$	[kW]	13.5% +/- 1.02 [kW]
Solar collector field heat produced	$\dot{Q}_{coll}$	[kW]	6% +/- 127 [W]
Hourly thermal COP	COP_{therm}	[-]	22.50%
Electrical power			
Hydraulics module (including three pumps) and chiller	$\dot{Q}e6$	[W]	1%
Solar loop pump power	$\dot{Q}e7$	[W]	10%
Cooling tower consumption	$\dot{Q}e8$	[W]	0.6%
Hot water tank electrical heating	$\dot{Q}e9$	[W]	5%
Meteorological data			
Collector field available solar energy	$\dot{Q}_{sol}$	[kW]	5%

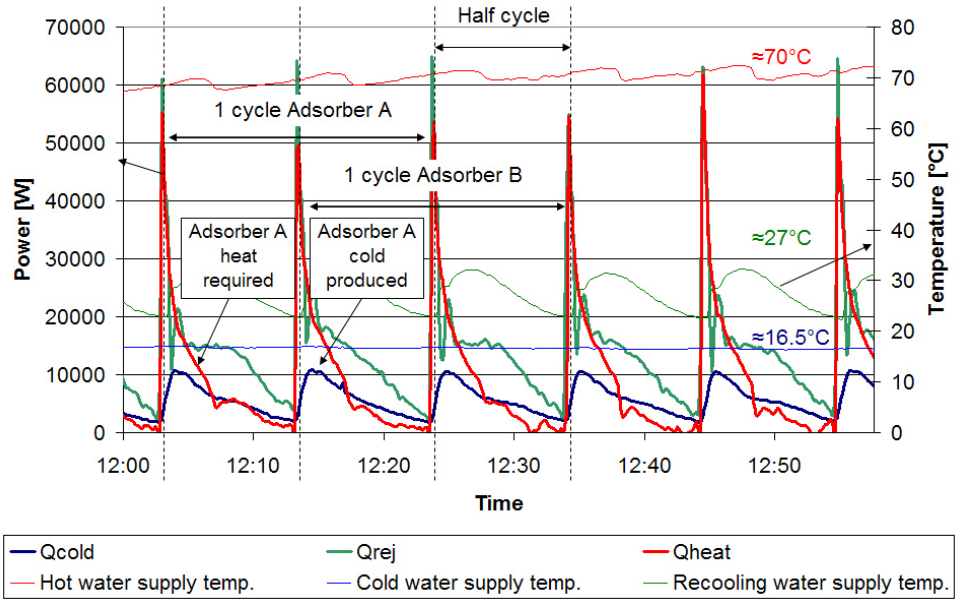

Figure 2: Heat flows in the adsorption chiller and three source/sink temperatures at midday on August 22nd

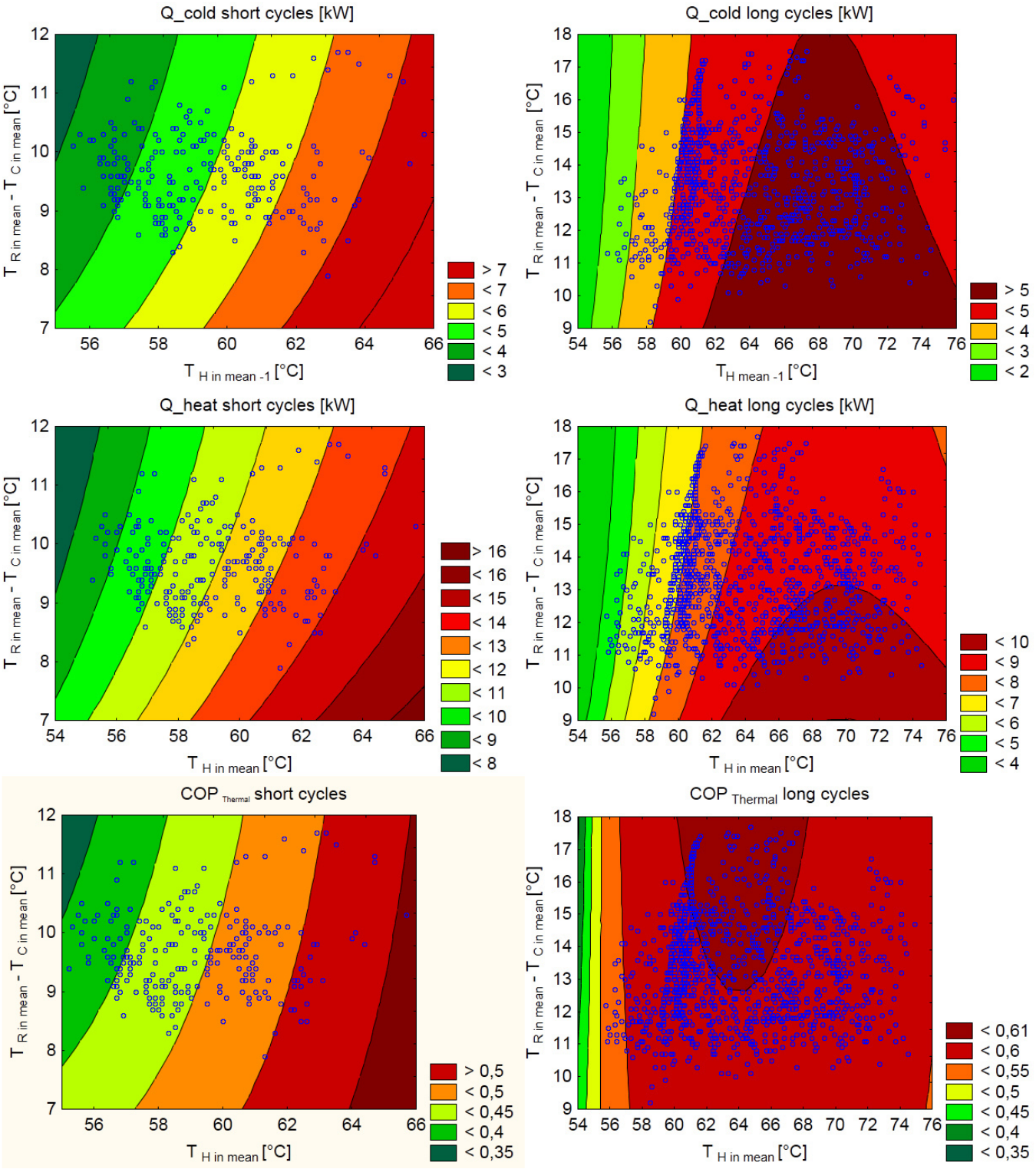

Figure 3: Steady-state model cold produced, heat consumed and thermal COP

Table 3: Steady-state model parameters and accuracy

	Long cycles		**Short cycles**	
Parameter	C	H	C	H
a	0.03153354	0.09881034	0.14329437	0.04119603
b	-0.90028281	-0.72086184	0.35737759	-2.89661804
c	0.08417317	0.07425552	0.01861709	0.02368329
d	18175.0991	25580.3242	-6314.46286	-166.50535
e	-565935.35	-790307.519	142685.278	-48950.7968
f	16.12863	30.7385458	28.8740547	37.3844624
g	-144.788189	-206.257837	67.1774599	23.8281952
Model accuracy	[kW]	[kW]	[kW]	[kW]
RMSE test data	0.172	0.299	0.273	0.603
RMSE all data	0.171	0.285	0.158	0.293
	[%]	[%]	[%]	[%]
Seasonal error	0.1	1.9	0.3	-1.8
Seasonal COP_{Therm} error	1.8		1.5	

Table 4: Steady-state model temperature validity ranges

Criteria	**Short cycles** $T_{C\,in\,mean} > 17°C$	**Long cycles** $T_{C\,in\,mean} \leq 17°C$
$T_{H\,in\,mean}$	55-65 °C	55-75 °C
$T_{R\,in\,mean}$	26-29 °C	26-29 °C
$T_{C\,in\,mean}$	17-19 °C	10-17 °C
$T_{R\,in\,mean} - T_{C\,in\,mean}$	8-12 °C	9-18 °C
$T_{H\,in\,max} - T_{H\,in\,min}$	$< 4°C$	$< 4°C$

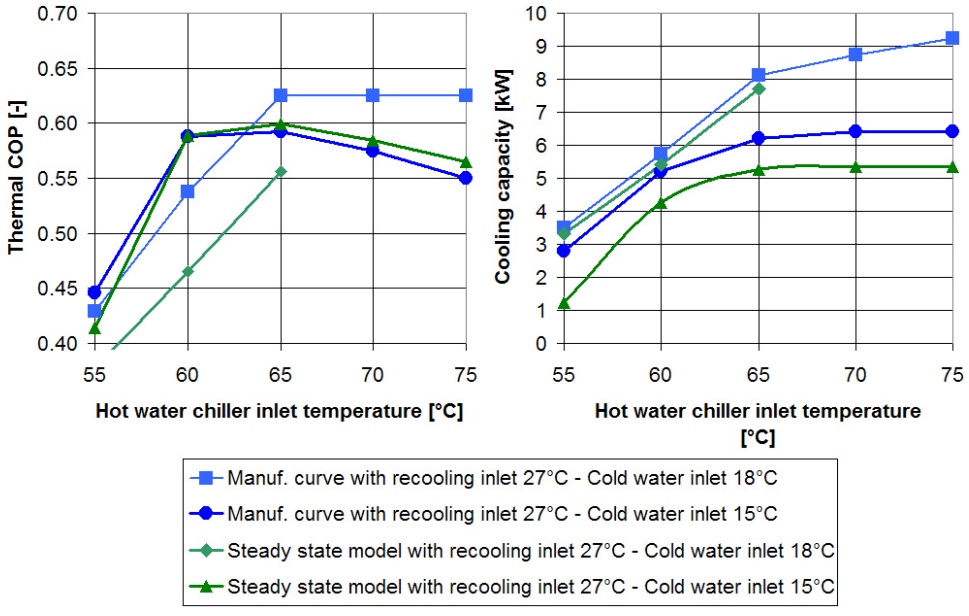

Figure 4: Manufacturer performance map comparison with steady-state model